



HAL
open science

INFLUENCE OF H₂S ON THE THERMAL CRACKING OF ALKYL BENZENES AT HIGH PRESSURE (70 MPa) AND MODERATE TEMPERATURE (583-623 K)

V. Burklé-Vitzthum, N.C. C Leguizamon Guerra, C. Lorgeoux, D.
Faure-Catteloin, R. Bounaceur, R. Michels

► **To cite this version:**

V. Burklé-Vitzthum, N.C. C Leguizamon Guerra, C. Lorgeoux, D. Faure-Catteloin, R. Bounaceur, et al.. INFLUENCE OF H₂S ON THE THERMAL CRACKING OF ALKYL BENZENES AT HIGH PRESSURE (70 MPa) AND MODERATE TEMPERATURE (583-623 K). *Journal of Analytical and Applied Pyrolysis*, 2019, 140, pp.423-433. 10.1016/j.jaap.2019.04.025 . hal-02370894

HAL Id: hal-02370894

<https://hal.science/hal-02370894v1>

Submitted on 19 Nov 2019

HAL is a multi-disciplinary open access archive for the deposit and dissemination of scientific research documents, whether they are published or not. The documents may come from teaching and research institutions in France or abroad, or from public or private research centers.

L'archive ouverte pluridisciplinaire **HAL**, est destinée au dépôt et à la diffusion de documents scientifiques de niveau recherche, publiés ou non, émanant des établissements d'enseignement et de recherche français ou étrangers, des laboratoires publics ou privés.

INFLUENCE OF H₂S ON THE THERMAL CRACKING OF ALKYL BENZENES AT HIGH PRESSURE (70 MPa) AND MODERATE TEMPERATURE (583-623 K)

V. Burklé-Vitzthum^{a*}, N. C. Leguizamon Guerra^{a,b}, C. Lorgeoux^b, D. Faure-Catteloin^b, R. Bounaceur^a, R. Michels^b

^a Laboratory of Reactions and Process Engineering, LRGP UMR 7274, CNRS, Université de Lorraine BP 20451, 54001 Nancy, France

^b GeoRessources UMR 7359, CNRS, Université de Lorraine BP 70239, 54501 Vandœuvre-lès-Nancy, France

* Corresponding author. Tel.: +33372743816

E-mail address: valerie.vitzthum@univ-lorraine.fr (V. Burklé-Vitzthum).

Keywords: Pyrolysis; organosulfur compounds; high pressure; H₂S; alkylbenzene; kinetic effect; apparent kinetic parameters

Highlights

- Pyrolysis of *n*-butylbenzene/H₂S mixture (80 % : 20% mol) at 70 MPa and from 583 K to 623 K was performed in sealed gold tubes.
- The main products are toluene, ethylbenzene, iso-butylbenzene and hydrocarbon gases (C₁, C₂ and C₃).
- Several organosulfur compounds are produced: mainly short thiols, phenylbutanethiols, and phenylthiophenes.
- H₂S accelerates the pyrolysis of *n*-butylbenzene by a factor up to almost 4 depending on the experimental conditions.
- The molecular composition of the products is highly modified in the presence of H₂S.

Abstract

The thermal cracking of *n*-butylbenzene was experimentally studied in the presence of H₂S (80% : 20% mol) at high pressure (70 MPa), moderate temperature (583, 603 and 623 K) and for durations of 3, 7 and 15 days. The pyrolysis was performed in sealed gold tubes under isobaric conditions. Under these conditions, the conversion of *n*-butylbenzene varied between 2.5% and 73.2%. The pyrolysis of *n*-butylbenzene is accelerated by H₂S by a factor of up to 3.6 depending on the operating conditions. This acceleration factor seems to decrease with increasing time and temperature. The apparent activation energy of the pyrolysis of *n*-butylbenzene decreases from 66.6 kcal/mol (pure *n*-butylbenzene) to 55.9 kcal/mol (*n*-butylbenzene in mixture with H₂S). The main hydrocarbons produced are alkylbenzenes (mostly toluene and ethylbenzene), branched alkylbenzenes (mostly isomers of iso-butylbenzene and iso-heptylbenzene to a lesser extent) and short alkanes (from CH₄ to C₃). Several sulfur compounds are also produced and their relative abundances are in the range 4-16% depending on the operating conditions. These sulfur compounds are mostly short thiols (methanethiol, ethanethiol and propanethiols), phenylbutanethiols and phenylthiophenes. Additional experiments were also conducted with alkylbenzenes bearing shorter substituents than *n*-butylbenzene (toluene, ethylbenzene and *n*-propylbenzene) in order to highlight the influence of the length of the side chain. Finally, the kinetic effect of H₂S on the pyrolysis of *n*-butylbenzene was compared to its effect on *n*-octane pyrolysis: the effect seems antagonistic under the studied experimental conditions but some similarities can be highlighted.

1. Introduction

H₂S can be the dominant gas in hot (>100°C) carbonate petroleum reservoirs [1][2][3][4]. Its abundance in reservoirs is essentially linked to Thermochemical Sulfate Reduction (TSR) which is the reaction of hydrocarbons with sulfate in formation waters within rock strata (e.g. [5][6][7][8][9]) at T>100°C. TSR is one of the most important reactions detrimental to oil composition in petroleum reservoirs; it involves a complex reaction network that leads to the reduction of sulfate to H₂S and to the oxidation of hydrocarbons to CO₂ ([8][10]). The deficiency in available iron of carbonate reservoir

rocks prevents the precipitation of iron sulfides. Therefore, H₂S will accumulate in petroleum traps. Because of its deleterious effect on oil composition, as well as greater production risks and costs due to the toxicity and corrosiveness of H₂S and CO₂, TSR has been extensively studied in the literature (e.g. [10][11][12][13][14]). In experimental studies, much attention has been paid to the formation of H₂S and sulfur compounds arising from reaction within the water phase or at the interface with the hydrocarbon phase. Very few studies deal with the consequence of a direct reaction of H₂S on the hydrocarbons ([14] [15] [16] [17][18]) within the organic phase or at the oil-gas interface, especially in the absence of TSR conditions. Yet, such information would be of great value since an improved understanding of the fate of H₂S and organic sulfur compounds would be highly beneficial for petroleum exploration, exploitation of high sulfur petroleum fields, recovery of heavy oil by steam injection, enhanced recovery by gas injection and sequestration of H₂S in depleted petroleum reservoirs.

Up to now, published studies about the influence of H₂S on hydrocarbons concern either oils [18] or pure alkanes (*n*-octane or *n*-hexadecane) as model compounds ([14][15][16][17]). The reaction of H₂S in the presence of an alkane leads to organosulfur compounds that are mostly thiols, thiacycloalkanes and thiophenes, whereas naphthenoaromatic species with 1-3 S atoms are produced during the pyrolysis of oils in the presence of H₂S. Moreover, it has been shown that H₂S slightly inhibits the pyrolysis of *n*-octane at 70 MPa and 603-623 K and this result enabled the construction of a detailed kinetic model [17]. In the conversion range studied, no sulfur naphthenoaromatic species were produced from *n*-octane, although they are formed from oils. An assumption is that they may derive from aromatic compounds by pyrolysis in the presence of H₂S. Indeed petroleum contains about 20 to 60 weight % of aromatic hydrocarbons [19].

The purpose of this paper is to study the influence of H₂S on the pyrolysis of aromatic compounds. *N*-butylbenzene has been chosen as the model compound of the aromatic fraction as in several previous studies ([20][21][22][23]). The alkyl side chain is long enough to allow the possible production of polycyclic compound. A previous published paper presented the experimental results and the construction of the detailed kinetic model of the pyrolysis of pure *n*-butylbenzene [24]. Here the pyrolysis of the *n*-butylbenzene/H₂S (80% : 20% mol) mixture is investigated at 70 MPa and in the

range 583-623 K. The detailed results, *i.e.* product distribution, conversion and kinetic influence of H₂S, are presented, as well as some results for other aromatic compounds with H₂S as exploratory experiments: toluene, ethylbenzene and *n*-propylbenzene. This study may help in our understanding of the fate of sulfur species in petroleum reservoirs.

2. Experimental and analytical procedure

2.1. Samples

Toluene, ethylbenzene, *n*-propylbenzene and *n*-butylbenzene (purity $\geq 99\%$), were obtained from Sigma Aldrich and used as received. H₂S (purity $\geq 99.5\%$) was provided by Air Liquide.

2.2. Loading procedure and pyrolysis device

Confined pyrolysis of alkylbenzene (toluene, ethylbenzene, *n*-propylbenzene and *n*-butylbenzene) / H₂S mixtures with constant molar ratio of 80/20 was carried out in gold tubes (purity 99.99%, 10 cm length, 5 mm i.d. and 0.5 mm thickness). Each gold tube was prepared in two steps: first, 100 μ L of liquid *n*-butylbenzene were loaded in using a syringe; then, following the procedure developed by Jacquemet et al. [25], 160 μ mol of H₂S were liquefied into the gold tube plunged in a liquid nitrogen bath. The gold tubes were maintained frozen under a cold nitrogen flow while sealed by pulse arc-welding and then placed in a pressurized autoclave at 70 MPa. Details on the confined pyrolysis procedure can be found in [26] and [27]. Suitability of confined pyrolysis for the study of thermal evolution of kerogen and hydrocarbons in petroleum systems and sedimentary basins was discussed elsewhere ([28][29]). In the case of *n*-butylbenzene, nine reaction sets, composed of four tubes each, were pyrolyzed at 583 K, 603 K and 623 K (± 1 K) for durations of 3, 7 and 15 days. These experiments were used for quantification and mass balance calculations. An additional experiment was conducted at 623 K for 15 days and used for the identification of reaction products. Pyrolysis was quickly stopped by using a water heat exchanger to cool the autoclaves to room temperature.

For the mixtures of toluene, ethylbenzene or *n*-propylbenzene / H₂S, only one experimental condition was studied: 70 MPa, 623 K and 7 days.

2.3. Identification of products

Gas products (C_1 - C_4) of the pyrolysis of the *n*-butylbenzene / H_2S mixture were identified by comparison of chromatographic retention times with those of a certified mixture (Air Products). Thermodesorption-GC-FID was used for this purpose. Principles of the technique are described in [30]. A gas sample of 10 μ L was directly injected by a Valco pneumatic valve into a Zebron ZB 5-MS column (Phenomenex, length: 60 m, 0.25 mm i.d., 0.10 μ m film). The chromatographic column was installed in a GC- Shimadzu 2010 Plus (carrier gas H_2) equipped with a cryogenic focus temperature controller (Frontierlab MJT 1035E) and a Flame Ionization Detector (FID). The GC-FID temperature program started at 303 K and was kept stable for 4 min, then a heating rate of 6 K/min was applied up to 593 K, and the final temperature was maintained during 10 min. The cryogenic focus froze the top of the column at 78 K during the first 2 minutes of the chromatographic program enhancing the separation of the light hydrocarbons (from C_1 to C_4).

The identification of the liquid products was performed by gas chromatography coupled to mass spectrometry (GCMS). A gold tube plunged in a beaker containing 10 mL dichloromethane was carefully opened from both ends. The solution and the gold tube were transferred into a vial and extracted in an ultrasonic bath during 1 hour. After rinsing of the gold tube, the recovered solution volume was normalized to 25 mL with a graduated flask, then 1 μ L of solution was analyzed by GC-MS (Shimadzu GCMS-QP 2010 Plus; carrier gas: He) using a Zebron ZB 5-MS column (Phenomenex, length: 60 m, 0.25 mm i.d., 0.10 μ m film, 5%-Phenyl, 95%-dimethylpolysiloxane phase). The temperature program was set as follows: the initial temperature was set at 313 K during 3.5 min, then a heating rate of 6 K/min was applied up to 593 K and final temperature was kept 10 min.

2.4. Quantification of products

The pyrolysis products of the *n*-butylbenzene/ H_2S mixture were quantified by Thermodesorption-GC-FID using the method described in [24]. The gold tubes were desorbed at 523 K inside a sealed piercing device under vacuum. An aliquot of remaining reactant and reaction products in the gas phase

was directly injected by a Valco pneumatic valve into the Zebron ZB 5-MS column. Gas compounds were calibrated from 0.28 μmol to 59.89 μmol using a certified bottle containing normal alkanes from methane to pentane (Air Products: Ar: 14.9600%; CO_2 : 24.9800%; CH_4 : 30.0300%; C_2H_6 : 13.0400%; C_3H_8 : 8.9660%; C_4H_{10} : 7.0240%; C_5H_{12} : 1.0022%). Liquid compounds from C_6 to C_{14} (29 compounds) were calibrated in the range 0.05 μmol - 14.20 μmol using solutions prepared with commercially available molecules (Fluka, Acros Organic, SigmaAldrich, Techlab). An external calibration curve of 6 concentrations was established for each compound. Every week the calibration mixtures were injected to verify the quality of detector response.

The quantification of the liquid sulfur compounds was performed by gas chromatography using parallel detection by FID and FPD (GC-FID-FPD, Agilent Technologies 7890 A). The calibration of the sulfur compounds detected by the FPD was performed with a solution of 21 compounds (thiols, thiophenes, benzothiophenes and dibenzothiophenes). The concentration range used for the calibrated compounds started at 1.19×10^{-2} $\mu\text{mol/mL}$ up to 5.45×10^{-1} $\mu\text{mol/mL}$. Prior to injecting, 1-decanethiol ($\text{C}_{10}\text{H}_{21}\text{SH}$) was added to the calibration as well as to the sample solutions to be used as internal standards of FPD quantification. 1-Decanethiol was not produced by pyrolysis and did not co-elute with any of the pyrolysis products. The internal calibration curve with 7 concentration levels was determined for each compound. For the quantification of the sulfur compounds, the pyrolyzed gold tubes were extracted as described in subsection 2.3. After the addition of the internal standard, a 1 μL aliquot was injected in splitless mode and analyzed by GC-FID-FPD. The column and the chromatographic program of the GC-FID-FPD are similar to those used for the identification of liquid products by GC-MS in subsection 2.3.

Unreacted *n*-butylbenzene, and major pyrolysis products, toluene, 1-methylpropylbenzene, 2-methylpropylbenzene and 1-propylbutylbenzene, were present in high concentrations for several pyrolysis conditions making impossible their quantification by Thermodesorption-GC-FID. Therefore these compounds were quantified by FID detection using the Agilent 7890 A GC-FID-FPD and using a known dilution of the extracted solutions. An internal standard (*n*- $\text{C}_{20}\text{H}_{42}$) was added before injection. *n*- C_{20} was chosen for this study because it is not a reaction product and nor does it co-elute

with any product. An internal calibration curve of 7 concentration levels (from 1.19×10^{-5} $\mu\text{mole}/\mu\text{L}$ to 2.11×10^{-4} $\mu\text{mole}/\mu\text{L}$) was constructed for each compound. Calibration reliability of the FID and FPD detectors was tested by injection of control solutions after every 10 samples analyzed. The standard deviation is usually less than 10%, except for the very low concentrations for which it is much higher (Supplementary materials 1 and 2).

For the other mixtures (toluene, ethylbenzene, *n*-propylbenzene / H_2S), only the liquid sulfur products were analyzed, not the gas, nor the liquid hydrocarbon products.

3. Experimental results (pyrolysis of the *n*-butylbenzene / H_2S mixture)

The detailed experimental results are given as Supplementary Materials 1 and 2.

3.1. Conversion

The conversion of *n*-butylbenzene has been calculated by carbon balance, according to Eq. (1):

$$\text{Conversion of butylbenzene} = \frac{\sum_i N_i \times n_i}{10 \times n_{BB}^0} \quad (1)$$

Where N_i is the number of carbon atoms in the product i , n_i the amount (in moles) of i and n_{BB}^0 the initial amount (in moles) of *n*-butylbenzene.

Indeed, the quantification of the remaining *n*-butylbenzene was not precise enough to allow the calculation of the conversion, especially at low values. That is why the conversion of *n*-butylbenzene has been based on the products, except at high reaction advancement (623 K and 15 days) for which the conversion has been calculated with remaining *n*-butylbenzene (Eq. (2)).

$$\text{Conversion of butylbenzene} = \frac{n_{BB}^0 - n_{BB}}{n_{BB}^0} \quad (2)$$

Where n_{BB} is the amount (in moles) of remaining *n*-butylbenzene.

Table 1. Conversion of *n*-butylbenzene and carbon balance after pyrolysis in the presence of 20 mol% H₂S at 70 MPa.

Temperature (K)	Time (days)	Conversion (%)	Carbon balance (%)
583	3	2.5 ± 0.2	104 ± 5
	7	3.2 ± 0.1	101 ± 5
	15	5.2 ± 0.2	101 ± 5
603	3	6.0 ± 0.1	107 ± 6
	7	8.3 ± 0.2	101 ± 7
	15	24.6 ± 0.4	109 ± 5
623	3	26.9 ± 0.3	99 ± 5
	7	47.7 ± 0.1	107 ± 8
	15	73.2 ± 0.3	86 ± 5

The conversion (Table 1) is in the range 2.5 % (at 583 K, 3 days) – 73.2% (at 623 K, 15 days).

The carbon balance *C.B* has been calculated according to Eq. (3):

$$C.B = \frac{\sum_i N_i \times n_i + 10 \times n_{BB}}{10 \times n_{BB}^0} \quad (3)$$

The carbon balance (Table 1) is between 86% and 109% and the mean value is 102%. These results are globally satisfying considering that the quantification procedure combines two sampling methods and two analytical devices. At high conversion, the carbon balance is only 86%, which is probably due to the great number of products in this case. The quantification of all of them is difficult.

The conversion of H₂S has been estimated by Eq. (4). The sulfur balance could not be verified because the remaining H₂S could not be quantified with the analytical tools used. That is why the conversion of H₂S can only be estimated and its values should be considered with caution.

$$\text{Conversion of } H_2S = \frac{\sum_i n_{jSC}}{n_{H_2S}^0} \quad (4)$$

Where $n_{H_2S}^0$ is the initial amount (in moles) of H₂S and n_{jSC} the amount (in moles) of the sulfur compound j.

It should be noted that all identified sulfur compounds only contain one sulfur atom. The estimated conversion of H₂S (Table 2) is in the range 1.9% (at 583 K, 3 days) – 17.8% (at 623 K, 7 days). The maximum conversion of H₂S is about 4 times lower than the conversion of *n*-butylbenzene. The decrease of the conversion between 7 days and 15 days at 623 K is probably not significant, according to the high error-bar at 623 K – 15 days.

Table 2. Estimated conversion of H₂S after pyrolysis of H₂S-butylbenzene mixture at 70 MPa.

Temperature (K)	Time (days)	Conversion (%)
583	3	1.9 ± 0.1
	7	2.2 ± 0.3
	15	2.6 ± 0.1
603	3	3.3 ± 0.4
	7	4.7 ± 0.4
	15	8.1 ± 4.0
623	3	12.3 ± 1.5
	7	17.8 ± 1.5
	15	17.0 ± 5.1

3.2. Product distributions

The hydrocarbons produced by the pyrolysis of *n*-butylbenzene/H₂S mixture are globally the same than those obtained by the pyrolysis of pure *n*-butylbenzene [24]: short alkylbenzenes (toluene, ethylbenzene), branched alkylbenzenes (iso-butylbenzenes, iso-heptylbenzenes), alkenylbenzenes (styrene, butenylbenzenes), gaseous products (from methane to butane) and methylindane. Typical gas chromatograms obtained for gaseous and liquid products can be seen in [24].

The relative abundance of sulfur compounds S_{SC} has been defined by Eq. (5):

$$S_{SC} = \frac{\sum_j n_{jSC}}{\sum_i n_{iHC} + \sum_j n_{jSC}} \quad (5)$$

Where n_{iHC} is the amount (in moles) of the produced hydrocarbon i , and n_{jSC} the amount (in moles) of the produced sulfur compound j .

Table 3 shows the relative abundance of sulfur compounds. It appears clearly that it decreases as the time and temperature decrease: its value is equal to almost 16% at 583 K and 3 days, but only to 4% at 623 K and 15 days. This means that 84% of the products are purely hydrocarbons at low conversion and 96% at high conversion.

Table 3. Total relative abundance of sulfur products as a function of time and temperature obtained after pyrolysis of H₂S-butylbenzene mixture at 70 MPa.

Relative abundance of sulfur products (%)		Temperature (K)		
		583	603	623
Time (days)	3	15.8 ± 1.0	11.0 ± 1.4	7.8 ± 1.6
	7	14.2 ± 2.7	10.6 ± 0.5	6.2 ± 0.3
	15	10.5 ± 0.4	5.9 ± 1.2	4.2 ± 1.0

The distribution of the liquid sulfur products can be seen in Fig. 1. Several families of sulfur compounds have been identified: short thiols (methanethiol, ethanethiol and propanethiols), branched thiophenes, thiophenol, phenylbutanethiols, phenylthiophenes and some branched isomers, and polycyclic sulfur compounds. At high conversion, the most abundant sulfur compounds are in decreasing order of concentration: 2-phenylthiophene, propanethiols, methanethiol, 3-phenylthiophene and benzylthiophenes.

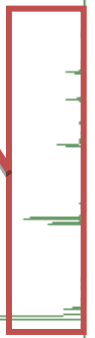
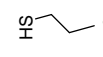
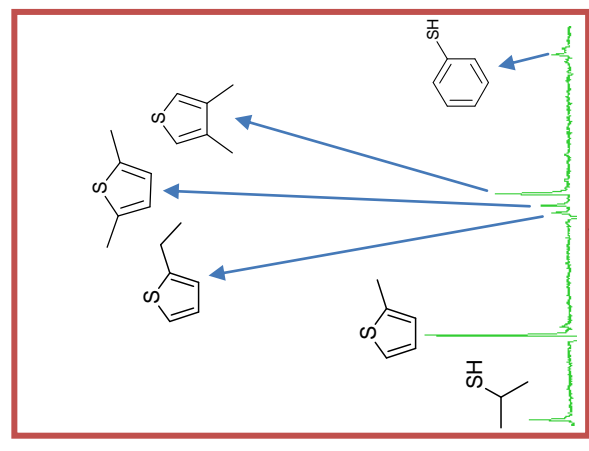
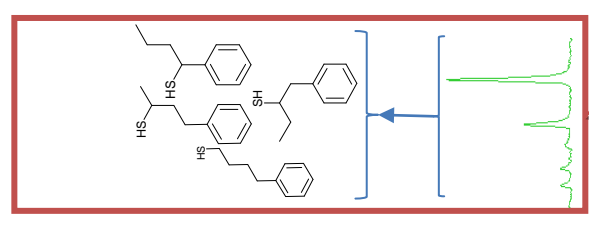
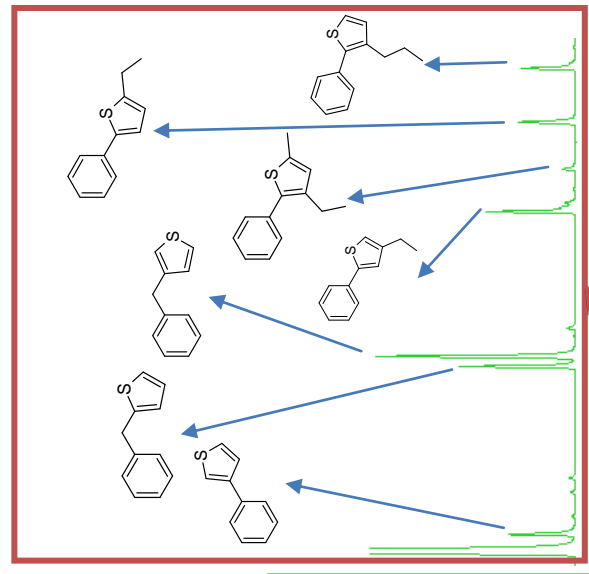
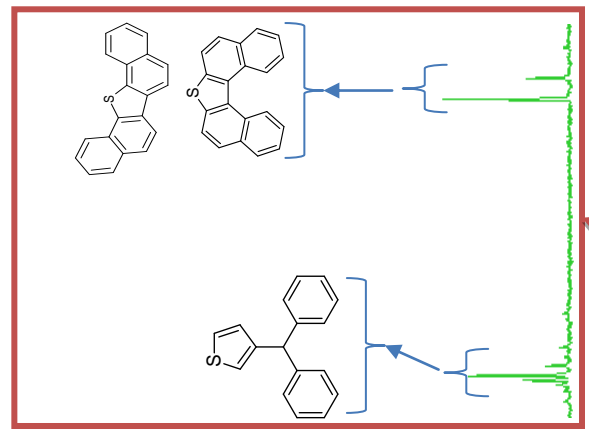
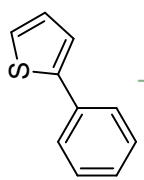


Figure 1. GC-FPD obtained after pyrolysis of the *n*-butylbenzene/H₂S mixture (70 MPa, 623 K, 15 days). The FPD does not detect the hydrocarbons, but only the sulfur species.

4. Kinetic effect of H₂S on *n*-butylbenzene thermal cracking

The conversion of *n*-butylbenzene in mixture with H₂S is compared to the conversion of pure *n*-butylbenzene [24] (Fig. 2). It appears that H₂S increases *n*-butylbenzene conversion in every studied operating condition: H₂S accelerates the pyrolysis of *n*-butylbenzene at 70 MPa, in the range 583-623 K. In order to quantify this acceleration effect, the ratio of the conversion of *n*-butylbenzene in mixture to the conversion of pure *n*-butylbenzene has been calculated (Table 4).

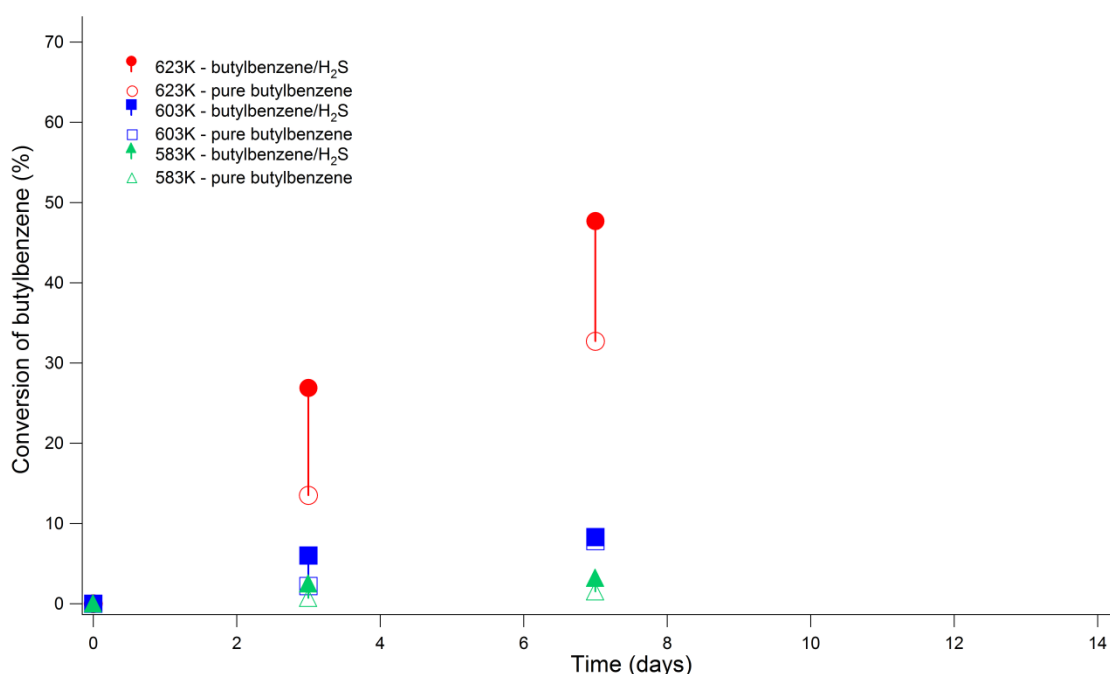


Figure 2. Conversion (%) of *n*-butylbenzene obtained by pyrolysis at 70 MPa, 523-623 K for 3 to 15 days duration: comparison between pure *n*-butylbenzene and *n*-butylbenzene/H₂S (80% : 20% mol) mixtures (vertical lines highlight the gap between the two systems at each temperature).

Table 4. Ratio of the conversion of *n*-butylbenzene in mixture with H₂S to the conversion of pure *n*-butylbenzene (70 MPa, 583-623 K, 3-15 days).

Conversion of butylbenzene in mixture with H ₂ S / Conversion of pure butylbenzene		Temperature (K)		
		583	603	623
Duration (days)	3	3.6	2.7	2.0
	7	2.2	1.1	1.5
	15	2.6	2.3	1.3

No monotonic trend can be highlighted for the acceleration effect of H₂S on *n*-butylbenzene pyrolysis. Nevertheless, it seems that the acceleration effect of H₂S decreases when duration and temperature increase.

The apparent kinetic parameters for the pyrolysis of *n*-butylbenzene in mixture with H₂S were calculated. The assumption of first-order kinetics allows computation of the rate constant by plotting $\ln(1 - \text{butylbenzene conversion})$ as a function of *time* (Table 5). The calculation of each rate constant requires the use of the three experimental conversions per temperature that were measured.

Table 5. Apparent rate constant (day⁻¹) for the pyrolysis of *n*-butylbenzene in mixture with H₂S.

Temperature (K)	Apparent rate constant k (day ⁻¹)	R ²
583	0.004	0.72
603	0.018	0.95
623	0.089	0.99

According to the Arrhenius law, the plot of $\ln k$ vs $1/RT$ (Fig. 3) allows the calculation of the apparent frequency factor A and the apparent activation energy E_a . E_a was found to be 55.9 kcal/mol and A to be $4.2 \times 10^{13} \text{ s}^{-1}$ for the *n*-butylbenzene/ H_2S mixture, whereas these values were 66.6 kcal/mol and $6.3 \times 10^{16} \text{ s}^{-1}$ respectively, for pure *n*-butylbenzene pyrolysis [24]. The significantly lower value of E_a in comparison to pure *n*-butylbenzene thus characterizes: 1) the global acceleration effect of H_2S on *n*-butylbenzene cracking, despite the lower value of A which decreases the rate constant to a lower extent than the increase due to the relatively low value of E_a 2) the higher acceleration effect of H_2S at 583 K than at 623 K.

The acceleration effect of organic sulfur compounds on hydrocarbon cracking is widely described in the literature ([31] [32]). Our results are the first to demonstrate the acceleration effect induced by H_2S which is notable, even at low degrees of advancement of the reaction. At higher degrees of advancement, the formation of organic sulfur compounds may also contribute to the acceleration. Indeed, labile organic sulfur compounds such as thiols have also been recognized as accelerators ([33][34][35][36][37][38]).

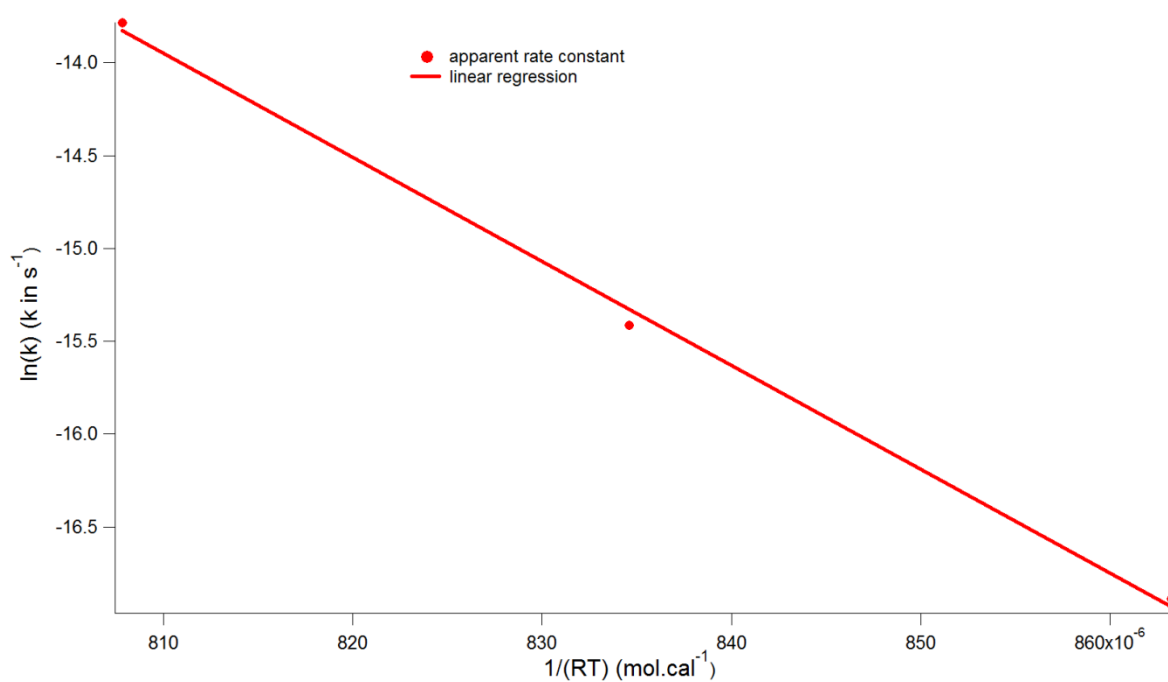


Figure 3. Plot of $\ln k$ as a function of $1/RT$ for the pyrolysis of *n*-butylbenzene in mixture with H₂S.

5. Comparison of product distributions

5.1. *n*-Butylbenzene/H₂S mixture vs. pure *n*-butylbenzene

The comparison of the pyrolysis product distributions between the *n*-butylbenzene/H₂S mixture and pure *n*-butylbenzene [24] focuses on hydrocarbons. As highlighted above, the hydrocarbons produced by the pyrolysis of *n*-butylbenzene/H₂S mixture are globally the same than those obtained by the pyrolysis of pure *n*-butylbenzene [24]. The major differences are the yields X_i , which are expressed by Eq. (6):

$$X_i = \frac{n_i}{n_{BB}^0} \quad (6)$$

Where n_i is the amount of the product i and n_{BB}^0 the initial amount of *n*-butylbenzene (in moles).

The yields of toluene, ethylbenzene, iso-butylbenzenes, butenylbenzenes and gaseous products are higher in the presence of H₂S than for the pyrolysis of pure *n*-butylbenzene, in agreement with the global acceleration of the pyrolysis with H₂S. On the contrary, the yield of iso-heptylbenzenes decreases in the presence of H₂S. The yield of methylindane increases with H₂S at 583 K, but decreases at 603 and 623 K. No clear trend can be highlighted for styrene. In order to quantify the effect of H₂S, the yield ratios of pyrolysis products obtained in the presence of H₂S to those obtained with pure *n*-butylbenzene have been calculated for the most important hydrocarbons. Table 6 shows the results, for the case of experiments at 623 K.

Table 6. *n*-butylbenzene/H₂S mixture to pure *n*-butylbenzene yield ratios calculated for major reaction products at 623 K and 70 MPa.

Compound	$\frac{X_i \text{ (pyrolysis of mixture)}}{X_i \text{ (pyrolysis of pure butylbenzene)}}$
----------	-------------------------------------------------------------------------------------------

	3 days	7 days	15 days
Toluene	9.7	2.2	1.1
Ethylbenzene	2.7	2.7	1.9
Iso-butylbenzenes	1.4	2.8	1.7
Iso-heptylbenzenes	0.3	0.2	0.1
Styrene	0.7	0.6	1.1
Butenylbenzenes	2.2	1.7	1.1
Methylindane	0.7	0.9	0.4
Methane	12	26	1.7
Ethane	1.3	1.0	1.6
Propane	15	16	14
Butane	1.3	1.4	2.6

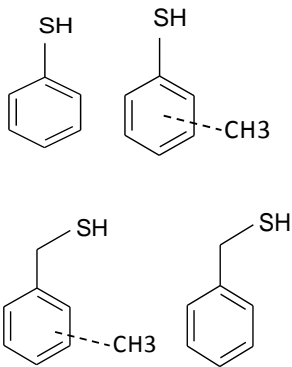
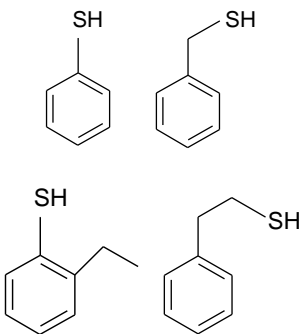
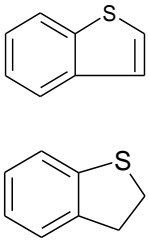
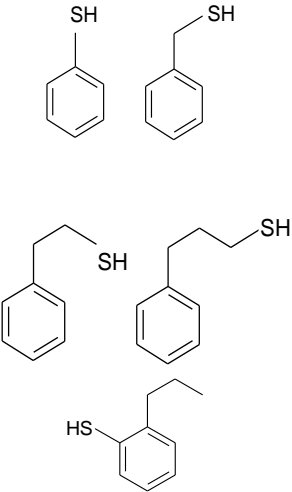
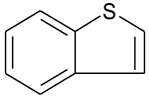
The results show that toluene, methane and propane are the most increased by H₂S. H₂S also increases the yields of ethylbenzene and iso-butylbenzenes in a significant manner. On the contrary, the formation of iso-heptylbenzene is strongly decreased by H₂S: the yield decreases by a factor of 3 to 9 and this effect increases with time. Iso-heptylbenzenes are mostly formed by addition of phenylbutyl radicals to propene [24]. The results obtained indicate that there is a competing reaction pathway in the presence of H₂S.

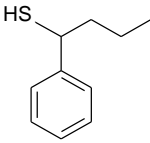
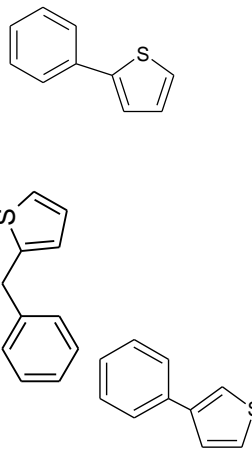
5.2. *n*-Butylbenzene/H₂S mixture vs. other alkylbenzene/H₂S mixtures

The distribution of the sulfur compounds obtained by pyrolysis of the *n*-butylbenzene/H₂S mixture is compared to those observed for other alkylbenzene (toluene, ethylbenzene and *n*-propylbenzene)/H₂S mixtures (80% : 20% mol). For these mixtures, only one condition was tested which is 623 K, 70 MPa and 7 days.

Table 7 compares the distribution of the sulfur compounds as a function of the length of the alkylbenzene side chain.

Table 7. Comparison of the distribution of the sulfur compounds as a function of the length of the alkylbenzene side chain after pyrolysis of the *n*-alkylbenzene/H₂S mixture at 623 K and 70 MPa.

Alkylbenzene	Aromatic thiols	Benzothiophenes	Aromatic thiophenes
Toluene			
Ethylbenzene		 <p>(traces)</p>	
Propylbenzene		 <p>(traces)</p>	

<p style="text-align: center;">Butylbenzene</p>	<p style="text-align: center;">Same products +</p> <div style="text-align: center;">  </div> <p style="text-align: center;">+ isomers</p>	<p style="text-align: center;">(traces)</p>	<div style="text-align: center;">  </div> <p style="text-align: center;">+isomers</p>
--------------------------------------------------------	----------------------------------------------------------------------------------------------------------------------------------------------------------------------------------------------------------------------------	---------------------------------------------	--------------------------------------------------------------------------------------------------------------------------------------------------------------------------

For every mixture, aromatic thiols have been identified. The length of the aromatic thiol side chain increases with the length of the alkyl substituent of the alkylbenzene. Except in the case of toluene for which the side chain is too short, traces of benzothiophenes have always been detected. Finally, 2- and 3-phenylthiophenes were found for the *n*-butylbenzene/H₂S mixture, but not for the other mixtures for which the side chains are shorter.

The yields X_i of the C₆⁺ sulfur compounds (in relation to the initial amount of alkylbenzene) are shown in Fig. 4 (pyrolysis at 623 K, 70 MPa and during 7 days). Aromatic thiols are the major sulfur products for toluene, ethylbenzene and *n*-propylbenzene, but the yield decreases by a factor of 4 in the case of *n*-butylbenzene compared to *n*-propylbenzene. At the same time, the total yield of sulfur compounds increases by a factor of almost 4 for *n*-butylbenzene compared to *n*-propylbenzene. Phenylthiophenes, which are not observed for shorter alkylbenzenes, become the major sulfur products in the pyrolysis of the *n*-butylbenzene/H₂S mixture.

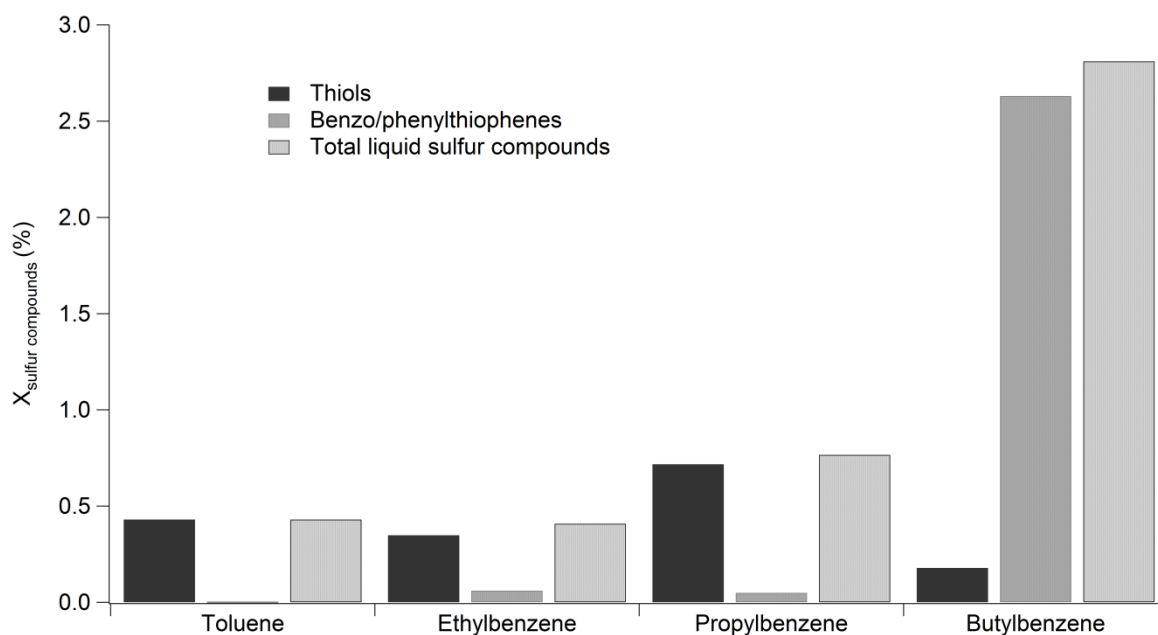


Figure 4. Yields X_i of thiols, benzothiophenes (for ethylbenzene and propylbenzene) or phenylthiophenes (for *n*-butylbenzene), and liquid sulfur compounds in relation to the initial amount of alkylbenzene. Pyrolysis of 80% alkylbenzene : 20% H_2S (mol) at 623 K, 70 MPa and during 7 days.

Note that the gaseous products were not analyzed except for the *n*-butylbenzene/ H_2S mixture. Therefore no comparison is possible, but in the case of *n*-butylbenzene, methanethiol, ethanethiol and propanethiol were quantified and represent about 20% of the sulfur compounds at high conversion (623 K and 15 days).

5.3. Possible reaction pathways

The aim of this part is to propose possible formation pathways for the sulfur compounds, by considering free-radical reactions.

The key free-radical for the production of organosulfur compounds is probably HS^\bullet which may be mostly formed by H-transfers between radicals derived from the pyrolysis of *n*-butylbenzene and H_2S (Fig. 5). The H-transfers with H_2S seem more favorable (higher rate constants) than with hydrocarbons [39] and they probably are predominant among all H-transfers.



Figure 5. Example of H-transfer between the 1-phenylbutyl radical and H₂S.

Except in the case of thiophenol, thiols may be produced by three pathways: additions of HS[•] to double bonds (Fig. 6) followed by H-transfers; terminations by recombination between HS[•] and radicals (Fig. 7); ipso-additions of radicals to H₂S (Fig. 8). Note that all these pathways compete with the additions of phenylbutyl radicals to propene that yield iso-heptylbenzenes. They may explain the decreasing concentration of iso-heptylbenzenes in the experiments conducted with H₂S in comparison to the pyrolysis of pure *n*-butylbenzene.

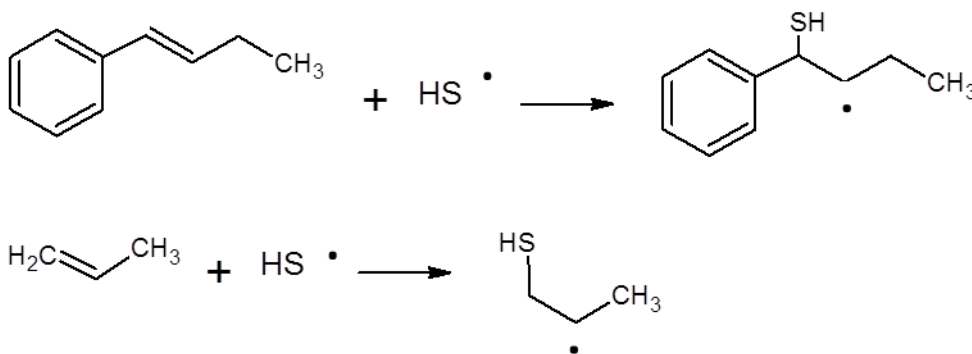


Figure 6. Examples of addition of HS[•] to butenylbenzene and propene.

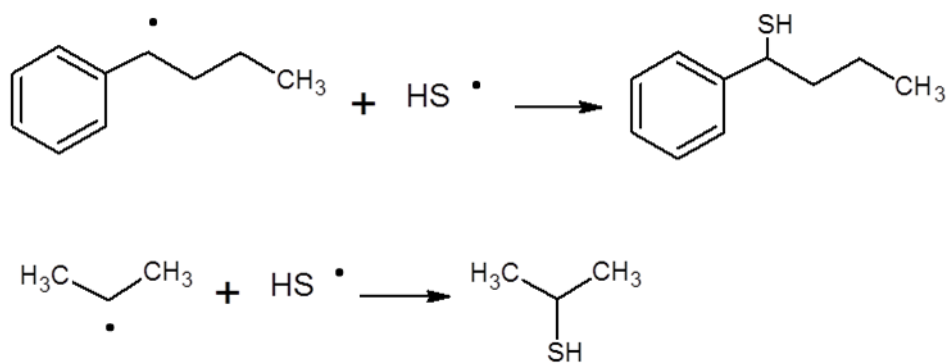


Figure 7. Examples of termination by recombination between HS[•] and 1-phenylbutyl radical, and between HS[•] and propyl radical.

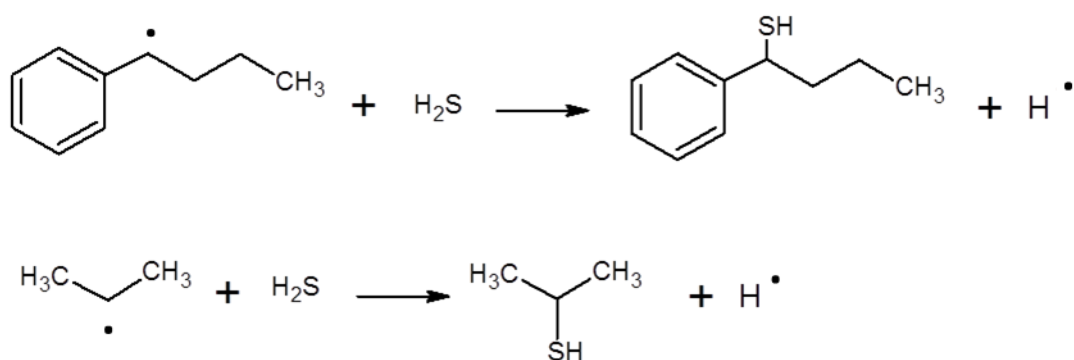


Figure 8. Examples of ipso-addition of 1-phenylbutyl and propyl radicals to H₂S.

Thiophenol might be produced by termination reactions implying recombination between HS[•] and the phenyl radical as well as ipso-addition of the phenyl radical to H₂S. Yet, the concentration of the phenyl radical is negligible [24]. Thiophenol may also be produced by ipso-addition of HS[•] to alkylbenzene (Fig. 9), in the same way as for H[•] or CH₃[•] [40].

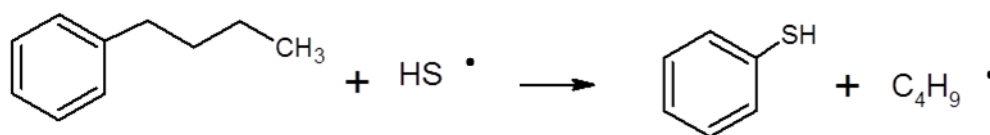


Figure 9. Example of ipso-addition of HS^\bullet to *n*-butylbenzene.

Phenylthiophenes may derive from phenylbutanethiols. Indeed, they are produced only in the case of the pyrolysis of *n*-butylbenzene/ H_2S and not for the shorter alkylbenzenes. Moreover phenylbutanethiols are less concentrated than their shorter alkylbenzene homologs, which may indicate a consumption pathway for these compounds. Two pathways can explain the formation of phenylthiophene. For the first pathway, the initial step may be the formation of a radical by H-transfer, then an internal ipso-addition of the single electron to the $-\text{SH}$ group yielding a bicyclic molecule, and finally aromatization by successive H-transfers and decompositions by β -scission leading to the phenylthiophenes (Fig. 10). For the second pathway, the first step may be the formation of a phenylbutenethiol, followed by the formation of a sulfured radical, an intramolecular addition, and finally aromatization (Fig. 11).

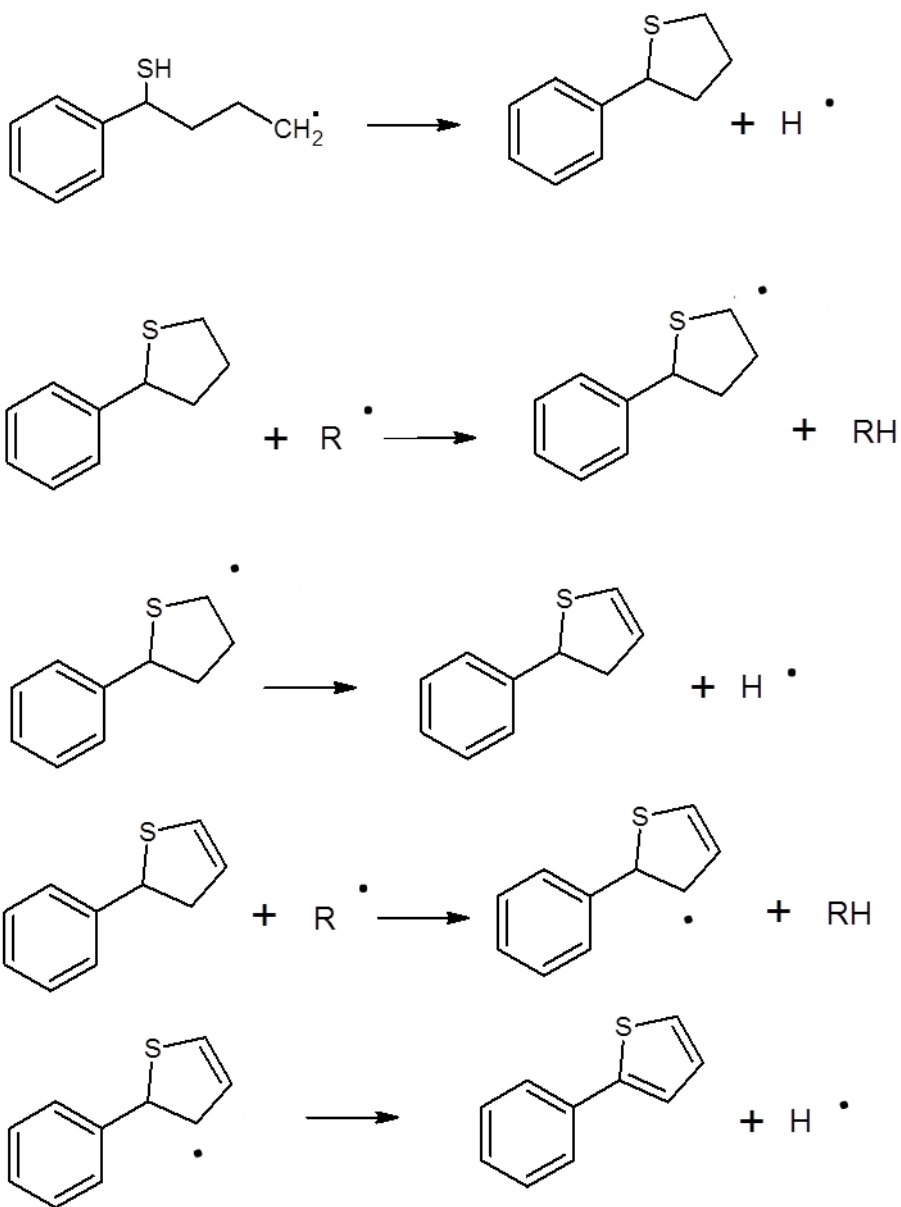


Figure 10. First proposed pathway for the formation of 2-phenylthiophene from butanethiol.

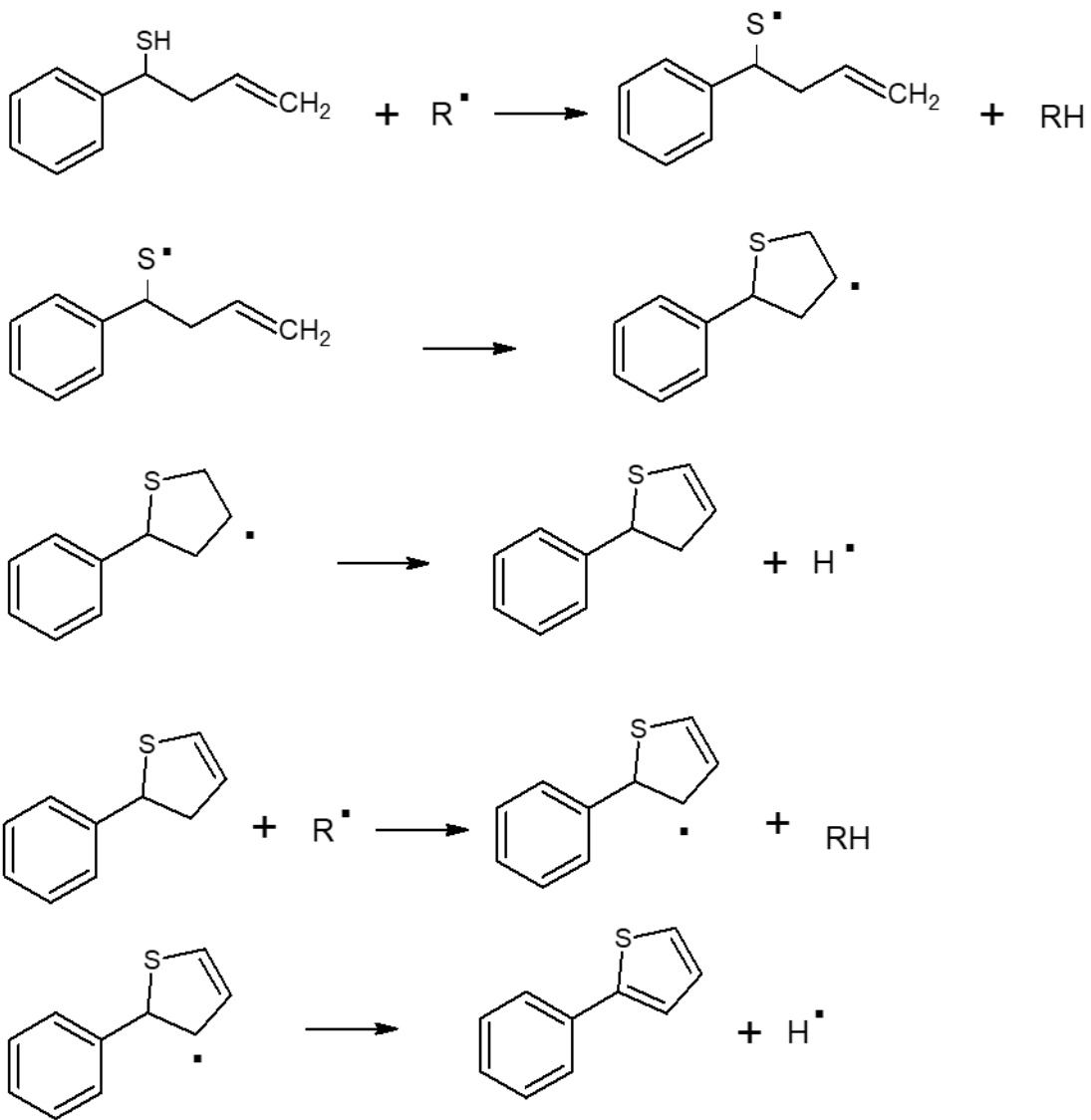


Figure 11. Second proposed pathway for the formation of 2-phenylthiophene from butenethiol.

Traces of benzothiophenes were detected for the pyrolysis of each alkylbenzene/H₂S mixture, except for toluene since the length of its alkyl substituent is too short to allow cyclisation. They may be produced by H-transfers from 2-phenylethanethiol, ring-closure reactions and decompositions by β-scission (Fig. 12).

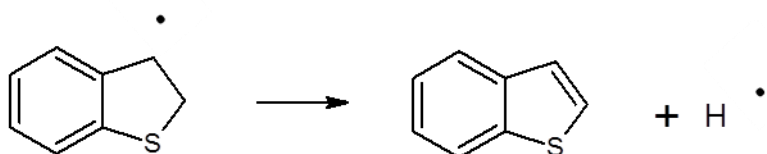
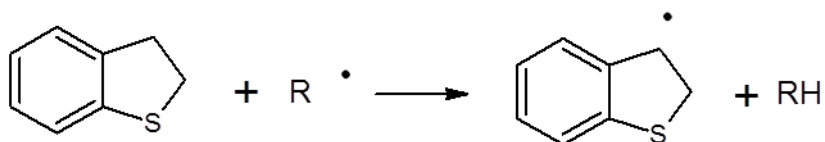
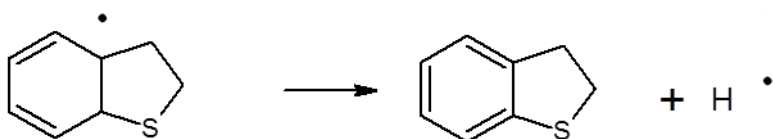
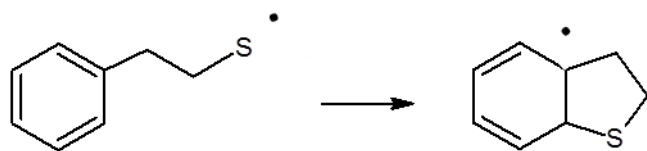
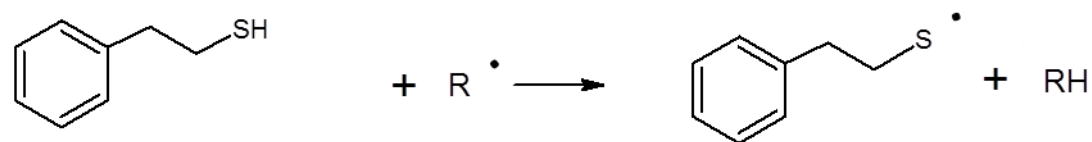


Figure 12. Proposed pathways for the formation of benzothiophene.

6. Kinetic effect of H₂S on *n*-butylbenzene thermal cracking – comparison with *n*-octane

As previously shown, H₂S has an acceleration effect on the pyrolysis of butylbenzene. However, the experimental study conducted by Nguyen et al. [17] on the *n*-octane/H₂S mixture showed an inhibition effect. Thus, the kinetic influence of H₂S depends on the nature of the hydrocarbon (*n*-alkane vs alkylaromatic), while the overall kinetics will depend on the competitive contributions of H₂S vs organo-sulfur compounds. Such dependency of the reaction rate on the initial nature of reactants as well as on composition changes of the system during pyrolysis might explain why the effects of sulfur compounds on the thermal cracking of petroleum lead to variable kinetic factor estimations [32].

Further understanding of the inhibition/acceleration effect induced by H₂S can be investigated by comparing the results of the *n*-butylbenzene/H₂S system to the *n*-octane/H₂S system obtained under the same operating conditions [17]. For the *n*-octane/H₂S mixture, the inhibition effect of H₂S increases when the temperature increases. A detailed kinetic model for the pyrolysis of the *n*-octane-H₂S mixture was previously constructed and validated at 70 MPa, 603-623 K and for durations ranging from 3 to 15 days (conversion up to 15% [17]). This kinetic model has been extrapolated to lower temperature and simulations have been performed using the software package CHEMKIN II [41] and more precisely SENKIN at constant pressure and temperature. The ratio of the conversion of *n*-octane in mixture with H₂S to the conversion of pure *n*-octane has been computed at 70 MPa, 10% conversion of pure *n*-octane and from 523 to 623 K (Fig. 13). The simulation results show that H₂S would become an accelerator for *n*-octane pyrolysis at temperatures below 573 K and that the acceleration effect would increase as the temperature decreases.

The experimental ratios of the conversion of *n*-butylbenzene in mixture with H₂S to the conversion of pure *n*-butylbenzene are also shown in Fig. 13. Despite the apparent opposing kinetic effects of H₂S on *n*-octane (inhibition) and *n*-butylbenzene (acceleration) at high temperature, the simulation results indicate that the kinetic effect of H₂S on *n*-octane and *n*-butylbenzene shows similar trends with temperature. Both trends decrease with increasing temperature, but there is a difference in the transition temperature between acceleration and inhibition (intersection with the “no kinetic effect” line in Fig. 13) that is shifted to higher temperature for *n*-butylbenzene.

In the case of *n*-octane-H₂S, the inhibition effect in the temperature range (583-623 K) is interpreted by the detailed kinetic model previously published [17]. It invokes three major reaction pathways with mutually antagonistic effects: 1) new terminations with HS[•] which decrease the pyrolysis rate; 2) new bimolecular initiations with H₂S which increase the pyrolysis rate 3) a new parallel propagation loop which increases the pyrolysis rate. The relative importance of each effect depends on temperature.

The case of *n*-butylbenzene/H₂S mixture will also require a complete study of reaction mechanism. A further step would be the study of the ternary system (*n*-butylbenzene/*n*-octane/H₂S). Indeed H₂S seems to accelerate the pyrolysis of *n*-butylbenzene as well as that of *n*-octane at geological reservoir temperatures. But it has been previously shown that alkylbenzenes and particularly toluene inhibit the pyrolysis of alkanes under all temperature conditions investigated ([42][43][44]). A study of these competing effects would be required. Nevertheless, it could be assumed that, if the H-transfers with H₂S are really predominant in the system, the inhibition effect of alkylbenzenes on alkane pyrolysis would be suppressed in the presence of H₂S.

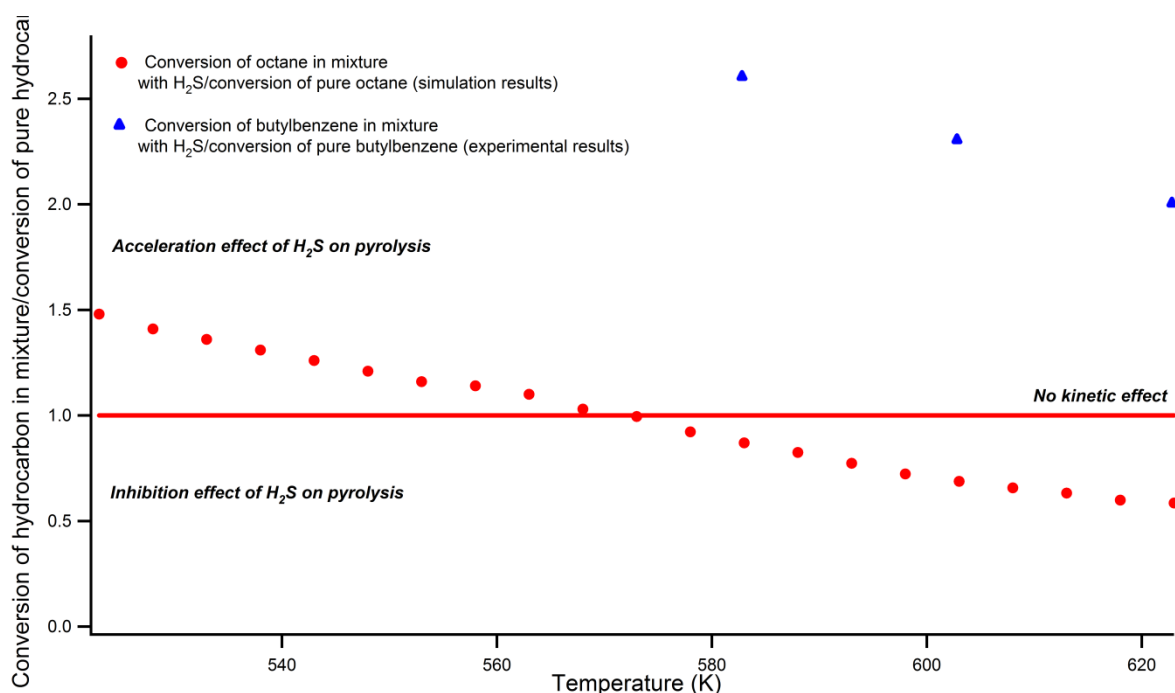


Figure 13. Comparison between the ratio of the conversion of *n*-octane in mixture with H₂S to the conversion of pure *n*-octane, and the ratio of the conversion of *n*-butylbenzene in mixture with H₂S to the conversion of pure *n*-butylbenzene. For *n*-octane: simulation results at 70 MPa and 10%

conversion of pure *n*-octane. For *n*-butylbenzene: experimental results at 70 MPa and 10% conversion of pure *n*-butylbenzene (except at 583 K: 2% conversion of pure *n*-butylbenzene).

7. Conclusion

The thermal cracking of *n*-butylbenzene was experimentally studied in the presence of H₂S (80% : 20% mol) at high pressure (70 MPa), moderate temperature (583, 603 and 623 K) and for durations of 3, 7 and 15 days. The pyrolysis was performed in sealed gold tubes in an isobaric regime. Under these conditions, the conversion of *n*-butylbenzene varies between 2.5% and 73.2%. H₂S accelerates the pyrolysis of *n*-butylbenzene by a factor up to 3.6 depending on the operating conditions in comparison with the pyrolysis of pure *n*-butylbenzene. This acceleration factor seems to decrease with increasing time and temperature. The apparent activation energy of the pyrolysis of *n*-butylbenzene decreases from 66.6 kcal/mol (pure *n*-butylbenzene) to 55.9 kcal/mol (*n*-butylbenzene in mixture with H₂S). A previous study has shown that H₂S has an inhibition effect on *n*-octane pyrolysis under the same operating conditions. Nevertheless, simulations of the pyrolysis kinetic model of the *n*-octane-H₂S mixture reveals that H₂S becomes an accelerator below 573 K and this acceleration effect increases as the temperature decreases. Thus, despite apparently contradictory behaviors, these results suggest that the kinetic effects of H₂S on *n*-octane and *n*-butylbenzene show a similar temperature dependence but the transition temperature between acceleration and inhibition is shifted to a higher temperature for *n*-butylbenzene.

The main hydrocarbons produced during the pyrolysis of the *n*-butylbenzene/H₂S mixture are alkylbenzenes (mostly toluene and ethylbenzene), branched alkylbenzenes (mostly isomers of iso-butylbenzene and iso-heptylbenzene to a lesser extent) and short alkanes (from CH₄ to C₃). Several sulfur compounds are also produced and their total relative abundance among the reaction products is in the range 4-16% depending on the operating conditions. These sulfur compounds are mostly short thiols (methanethiol, ethanethiol and propanethiols), phenylbutanethiols, and phenylthiophenes. Some additional experiments were also conducted with alkylbenzenes with a shorter alkyl chain than *n*-butylbenzene, in order to help elucidate the formation pathways of the sulfur compounds. Thus, formation pathways are proposed for the main sulfur compounds based on free-radical reactions.

The comparison of the results obtained by the pyrolysis of the *n*-octane/H₂S and the *n*-butylbenzene/H₂S systems highlights the kinetic effects of H₂S on hydrocarbon cracking. The inhibition/acceleration effects of H₂S depend on 1) the composition of the co-reactant (alkane vs alkyl-aromatic), 2) the temperature range, 3) the nature and abundance of the sulfur compounds generated during the reaction, 4) the presence of hydrocarbon species having their own kinetic influence on the mixture (e.g. toluene, long-chain-alkyl-aromatics, hydro-naphthalenics). The complex interdependence of these variables implies that the kinetic behavior of high sulfur oils, the calculation of the concentration of species of interest (like H₂S) and the understanding of reaction pathways must rely on reaction modelling.

Thus, the next step of this study will be the construction of a detailed kinetic model for the pyrolysis of *n*-butylbenzene/H₂S mixtures in order to identify the main reaction pathways and understand the kinetic effect of H₂S on *n*-butylbenzene pyrolysis.

Acknowledgements. This work was supported by ICEEL (Institut Carnot pour l'Energie et l'Environnement en Lorraine). We thank M. Aurelien Randi and M. Gilles Bessaque for their technical support.

References

- [1] G. A. Belenitskaya, Distribution pattern of hydrogen sulphide-bearing gas in former Soviet Union., *Petroleum Geoscience* (2000) 175-187.
- [2] G. H Isaksen, M. Khalylov, Controls on hydrogen sulfide formation in a Jurassic carbonate play, Turkmenistan, In P. O. Yilmaz and G. H. Isaksen, editors, *Oil and gas of the Greater Caspian area. AAPG studies in Geology* 55 (2007) 133-149.
- [3] C. Cai, R. Worden, G. A Wolff, S. Bottrell, D. Wang, X. Li, Origin of sulfur rich oils and H₂S in Tertiary lacustrine sections of the Jinxian Sag, Bohai Bay Basin, China, *Applied Geochemistry* (2015) 1427-1444.
- [4] G. Zhu, X. Liu , H. Yang, J. Su J., Y. Zhu, Y. Wang, C. Sun, Genesis and distribution of hydrogen sulfide in deep heavy oil of the Halahatang area in the Tarim Basin, China, *Journal of Natural Gas Geoscience* (2017) 99-108.

- [5] W.L. Orr, Changes in sulphur content and isotopic ratios of sulphur during petroleum maturation - Study of Big Horn Basin Paleozoic oils, *Am. Assoc. Petrol. Geol. Bull.* 58 (1974) 2295 - 2318.
- [6] H.R. Krouse, C.A. Viau, L.S. Eliuk, A. Ueda, S. Halas, Chemical and isotopic evidence of thermochemical sulphate reduction by light hydrocarbon gases in deep carbonate reservoirs, *Nature* 333 (6172) (1988) 415–419.
- [7] E. Heydari, C.H. Moore, Burial diagenesis and thermochemical sulfate reduction, Smackover Formation, southeastern Mississippi salt basin, *Geology* 17 (12) (1989) 1080-1084.
- [8] H.G. Machel, H.R. Krouse, R. Sassen, Products and distinguishing criteria of bacterial and thermochemical sulfate reduction, *Appl. Geochem.* 10 (4) (1995) 373-389.
- [9] R.H. Worden, P.C. Smalley, H₂S-producing reactions in deep carbonate gas reservoirs, Khuff Formation, Abu Dhabi, *Chem. Geol.* 133 (1–4) (1996) 157–171.
- [10] R.H. Worden, P.C. Smalley, H₂S in North Sea oil fields: importance of thermochemical sulphate reduction in clastic reservoirs, R. Cidu (Ed.), 10th International Symposium on Water-Rock Interactions, 2, Swets and Zeitlinger, Lisse (2001), 659-662.
- [11] B.K. Manzano, M.G. Fowler, H.G. Machel, The influence of thermochemical sulphate reduction on hydrocarbon composition in Nisku reservoirs, Brazeau river area, Alberta, Canada, *Org. Geochem.* 27 (7-8) (1997) 507-521.
- [12] C.F. Cai, R.H. Worden, S.H. Bottrell, L.S. Wang, C.C. Yang, Thermochemical sulphate reduction and the generation of hydrogen sulphide and thiols (mercaptans) in Triassic carbonate reservoirs from the Sichuan Basin, China, *Chem. Geol.* 202 (1–2) (2003) 39-57.
- [13] T. Zhang, G.S. Ellis, K.S. Wang, C.C. Walters, S.R. Kelemen, B. Gillaizeau, Y. Tang, Effect of hydrocarbon type on thermochemical sulfate reduction, *Org. Geochem.* 38 (2007) 897-910.

- [14] T. Zhang, A. Amrani, G.S. Ellis, Q. Ma, Y. Tang, Experimental investigation on thermochemical sulfate reduction by H₂S initiation, *Geochim. Cosmochim. Acta* 72 (14) (2008) 3518-3530.
- [15] A. Amrani, T. Zhang, Q. Ma, G.S. Ellis, Y. Tang, The role of labile sulphur compounds in thermochemical sulfate reduction, *Geochim. Cosmochim. Acta* 72 (12) (2008) 2960-2972.
- [16] V.P. Nguyen, V. Burkle-Vitzthum, P. M. Marquaire, R. Michels, Thermal reactions between alkanes and H₂S or thiols at high pressure, *J. Anal. Appl. Pyrolysis* 103 (2013) 307-319.
- [17] V. P. Nguyen, V. Burklé-Vitzthum, P.M. Marquaire, R. Michels, Pyrolysis mechanism of the n-octane/H₂S mixture at 70 MPa and 603-623K, *J. Anal. Appl. Pyrolysis*, 113 (2015) 46-56.
- [18] C.C. Walters, K. Qian, C. Wu, A.S. Mennito, A. Wei, Proto-solid bitumen in petroleum altered by thermochemical sulfate reduction, *Org. Geochem.* 42 (2011) 999-1006.
- [19] B.P. Tissot, D.H. Welte, *Petroleum Formation and Occurrence*; 2nd ed. Springer-Verlag: New-York (1984).
- [20] F. Dominé, High pressure pyrolysis of n-hexane, 2,4-dimethylpentane and 1-phenylbutane. Is pressure an important geochemical parameter? *Org. Geochem.* 17 (1991) 619-634.
- [21] C.H. Leigh, M.Szwarc, The pyrolysis of normal-butylbenzene and the heat of formation of normal-propyl radical, *J. Chem. Phys.* 20 (1952) 407-411.
- [22] H. Freund, W.N. Olmstead, Detailed chemical kinetic modeling of butylbenzene pyrolysis, *Int. J. Chem. Kinet.* 21 (1989) 561-574.

- [23] J. Yu, S. Eser, Thermal Decomposition of Jet Fuel Model Compounds under Near-Critical and Supercritical Conditions. 1. n-Butylbenzene and n-Butylcyclohexane, *Ind. Eng. Chem. Res.* 37 (1998) 4591-4600.
- [24] N.C. Leguizamon Guerra, J.C. Lizardo Huerta, C. Lorgeoux, R. Michels, R. Fournet, B. Sirjean, A. Randi, R. Bounaceur, V. Burklé-Vitzthum, Thermal cracking of n-butylbenzene at high pressure: Experimental study and kinetic modelling, *J. Anal. Appl. Pyrolysis* (2018) <https://doi.org/10.1016/j.jaap.2018.03.016>.
- [25] N. Jacquemet, J. Pironon, E. Caroli, A new experimental procedure for simulation of H₂S+CO₂ geological storage, *Oil & Gas Science and Technology* 60 (1) (2005) 193-206.
- [26] P. Landais, R. Michels, B. Poty, Pyrolysis of organic matter in cold-seal autoclaves. Experimental approach and application, *J. Anal. Appl. Pyrolysis* 16 (2) (1989) 103-115.
- [27] R. Michels, P. Landais, Artificial coalification – comparison of confined pyrolysis and hydrous pyrolysis, *Fuel* 73 (11) (1994) 1691-1696.
- [28] M. Monthioux, P. Landais, J.C. Monin, Comparison between natural and artificial maturation series of humic coals from the Mahakam delta, Indonesia. *Org. Geochem.* 8 (4) (1985) 275-292.
- [29] M. Monthioux, P. Landais, B. Durand, Comparison between extracts from natural and artificial maturation series of Mahakam delta coals. *Org. Geochem.* 10 (1-3) (1986) 299-311.
- [30] L. Gerard, M. Elie, P. Landais, Analysis of confined pyrolysis effluents by thermodesorption multidimensional gas chromatography, *J. Anal. Appl. Pyrolysis* 29 (2) (1994) 137-152.
- [31] A. K. Burnham, H. R. Gregg, R. L. Ward, K. G. Knauss, S. A. Copenhaver, J. G. Reynolds, R. Sanborn, Decomposition kinetics and mechanism of n-hexadecane-1,2-

- $^{13}\text{C}_2$ and dodec-1-ene-1,2- $^{13}\text{C}_2$ doped in petroleum and n-hexadecane, *Geochim. Cosmochim. Acta* 61 (1997) 3725-3737.
- [32] D. W. Waples, The kinetics of in-reservoir oil destruction and gas formation: constraints from experimental and empirical data, and from thermodynamics, *Org. Geochem.* 31 (6) (2000) 553-575.
- [33] A. R. Katritzky, R. Murugan, M. Balasubramanian, J. V. Greenhill, M. Siskin, G. Brons, Aqueous high-temperature chemistry of carbo- and heterocycles. Part 16. Model sulfur compounds: a study of hydrogen sulfide generation, *Energy Fuels* 5 (6) (1991) 823–834.
- [34] A. R. Katritzky, M. Balasubramanian, M. Siskin, Aqueous high-temperature chemistry of carbo- and heterocycles. 17. Thiophene, tetrahydrothiophene, 2-methylthiophene, 2,5-dimethylthiophene, benzo[b]thiophene, and dibenzothiophene, *Energy Fuels* 6 (4) (1992) 431–438
- [35] A. R. Katritzky, R. A. Barcock, M. Balasubramanian, J. V. Greenhill, Aqueous High-Temperature Chemistry of Carbo- and Heterocycles. 21. 1 Reactions of Sulfur-Containing Compounds in Supercritical Water at 460°C. *Energy Fuels* 8 (1994) 498-506.
- [36] M. Siskin, A. R. Katritzky, Reactivity of Organic Compounds in Superheated Water: General Background, *Chem. Rev.* 101 (2001) 825-835.
- [37] B. Yang, S. Tian, S. Zhao, A study of thermal decomposition of alkanethiols in pressure reactor, *Fuel Process. Tech.* 87 (8) (2006) 673-678.
- [38] F. Enguehard, S. Kressmann, F. Dominé, Kinetics of dibutylether pyrolysis at high pressure: Experimental study, *Org. Geochem.* 16 (1-3) (1990) 155-160.
- [39] Z. Zeng, M. Altarawneh, I. Oluwoye, P. Glarborg, B.Z. Dlugogorski, Inhibition and Promotion of Pyrolysis by Hydrogen Sulfide (H_2S) and Sulfanyl Radical (SH), *J. Phys. Chem. A* 120 (45) (2016) 8941-8948.

- [40] F. Lannuzel, R. Bounaceur, R. Michels, G. Scacchi, P-M. Marquaire, An extended mechanism including high pressure conditions (700 bar) for toluene pyrolysis, *J. Anal. Appl. Pyrolysis* 87 (2010) 236-247.
- [41] R.J. Kee, F.M. Rupley, J.A. Miller, Chemkin-II: A Fortran chemical kinetics package for the analysis of gas-phase chemical kinetics. Sandia National Laboratories, Livermore, CA, 1989.
- [42] V. Burklé-Vitzthum, R. Michels, G. Scacchi, P.M. Marquaire, D. Dessort, B. Pradier, O. Brevart, Kinetic effect of alkylaromatics on the thermal stability of hydrocarbons under geological conditions, *Org. Geochem.* 35 (2004) 3–31.
- [43] F. Lannuzel, R. Bounaceur, R. Michels, G. Scacchi, P.M. Marquaire, Reassessment of the Kinetic Influence of Toluene on n-Alkane Pyrolysis, *Energy Fuels* 24 (2010) 3817–3830.
- [44] R. Bounaceur, G. Scacchi, P.M. Marquaire, F. Dominé, O. Brevart, D. Dessort, B. Pradier, Inhibiting effect of tetralin on the pyrolytic decomposition of hexadecane. Comparison with toluene, *Ind. Eng. Chem. Res.* 41 (2002) 4689-4701.

List of table captions

Table 1. Conversion of *n*-butylbenzene and carbon balance after pyrolysis in the presence of 20 mol% H₂S at 70 MPa.

Table 2. Estimated conversion of H₂S after pyrolysis of H₂S-butylbenzene mixture at 70 MPa.

Table 3. Total relative abundance of sulfur products as a function of time and temperature obtained after pyrolysis of H₂S-butylbenzene mixture at 70 MPa.

Table 4. Ratio of the conversion of *n*-butylbenzene in mixture with H₂S to the conversion of pure *n*-butylbenzene (70 MPa, 583-623 K, 3-15 days).

Table 5. Apparent rate constant (day⁻¹) for the pyrolysis of *n*-butylbenzene in mixture with H₂S.

Table 6. *n*-butylbenzene/H₂S mixture to pure *n*-butylbenzene yield ratios calculated for major reaction products at 623 K and 70 MPa.

Table 7. Comparison of the distribution of the sulfur compounds as a function of the length of the alkylbenzene side chain after pyrolysis of the *n*-alkylbenzene/H₂S mixture between 583 and 623 K and 70 MPa.

List of figure captions

Figure 1. GC-FPD obtained after pyrolysis of the *n*-butylbenzene/H₂S mixture (70 MPa, 623 K, 15 days). The FPD does not detect the hydrocarbons, but only the sulfur species.

Figure 2. Conversion (%) of *n*-butylbenzene obtained by pyrolysis at 70 MPa, 523-623 K for 3 to 15 days duration: comparison between pure *n*-butylbenzene and *n*-butylbenzene/H₂S (80% : 20% mol) mixtures (vertical lines highlight the gap between both systems at each temperature).

Figure 3. Plot of $\ln k$ as a function of $1/RT$ for the pyrolysis of *n*-butylbenzene in mixture with H₂S.

Figure 4. Yields X_i of thiols, benzothiophenes (for ethylbenzene and propylbenzene) or phenylthiophenes (for *n*-butylbenzene), and liquid sulfur compounds in relation to the initial amount of alkylbenzene. Pyrolysis of 80% alkylbenzene : 20% H₂S (mol) at 623 K, 70 MPa and during 7 days.

Figure 5. Example of H-transfer between the 1-phenylbutyl radical and H₂S.

Figure 6. Examples of addition of HS[•] to butenylbenzene and propene.

Figure 7. Examples of termination by recombination between HS^\bullet and 1-phenylbutyl radical, and between HS^\bullet and propyl radical.

Figure 8. Examples of ipso-addition of 1-phenylbutyl and propyl radicals to H_2S .

Figure 9. Example of ipso-addition of HS^\bullet to *n*-butylbenzene.

Figure 10. First proposed pathway for the formation of 2-phenylthiophene from butanethiol.

Figure 11. Second proposed pathway for the formation of 2-phenylthiophene from butenethiol.

Figure 12. Proposed pathways for the formation of benzothiophene.

Figure 13. Comparison between the ratio of the conversion of *n*-octane in mixture with H_2S to the conversion of pure *n*-octane, and the ratio of the conversion of *n*-butylbenzene in mixture with H_2S to the conversion of pure *n*-butylbenzene. For *n*-octane: simulation results at 70 MPa and 10% conversion of pure *n*-octane. For *n*-butylbenzene: experimental results at 70 MPa and 10% conversion of pure *n*-butylbenzene (except at 583 K: 2% conversion of pure *n*-butylbenzene).